A SWAT modeling approach to assess the impact of climate change on consumptive water use in Lower Chenab Canal area of Indus basin

Usman Khalid Awan, Umar Waqas Liaqat, Minha Choi and Ali Ismaeel

ABSTRACT

Accurate assessment of spatio-temporal variations of consumptive water use (CWU) in large irrigation schemes is crucial for several hydrological applications. This study is designed to evaluate the impact of climate change on CWU in the Lower Chenab Canal (LCC) irrigation scheme of the Indus basin irrigation system of Pakistan. A distributed hydrological model, the soil and water assessment tool (SWAT), was spatially calibrated (2005–2009) and validated (2010–2012) for monthly CWU. The estimated CWU using the SWAT model showed promising results (the coefficient of determination (R^2) = 0.87 ± 0.06, Nash–Sutcliffe model efficiency (NSE) = 0.83 ± 0.06)) when compared with CWU determined by the Surface Energy Balance Algorithm (SEBAL) (R^2 = 0.87 ± 0.06, NSE = 0.83 ± 0.06). Future evaluation, performed by considering the representative concentration pathways (RCP) 4.5 and 8.5 climate change scenarios, showed that changes in temperature and rainfall would significantly influence the CWU in the LCC scheme. Compared with the reference period, annual water consumption in the basin would increase overall by 7% and 11% at the end of 2020 with monthly variations of –40% to 60% and –17% to 80% under RCP 4.5 and RCP 8.5 climate change scenarios, respectively. The water managers in the region have to consider this fluctuating consumptive use in water allocation plans due to climate change for better management of available water resources.

Key words | actual evapotranspiration, canal command area, climate change, SEBAL, SWAT

Usman Khalid Awan
Ali Ismaeel
International Center for Agricultural Research in the Dry Areas (ICARDA),
15 Khalid Abu Dalbouh St,
Abdoon EShamali,
PO Box 950764,
Amman,
Jordan

Umar Waqas Liaqat
Department of Civil and Environmental Engineering,
College of Engineering, Hanyang University,
Seoul 133-791,
Republic of Korea

Minha Choi (corresponding author)
Water Resources and Remote Sensing Laboratory,
Department of Water Resources,
Graduate School of Water Resources,
Sungkyunkwan University,
2066 Seobu-ro, Jangan-gu,
Suwon 440-746,
Republic of Korea
E-mail: *mhchoi@skku.edu*

INTRODUCTION

Climate change is one of the central driving forces affecting food and water resources at global scale (Brown & Funk 2008; Godfray *et al.* 2010; Yang *et al.* 2012). With increasing interest towards climate change adaption, there is a strong need to increase crop productions, specifically with limited water resources, in order to meet the current increasing food demands (Emam *et al.* 2015). On the other hand, the identification of climate change hotspots are also required for mitigating the adverse impacts of climate change on crop production (Yang *et al.* 2010). Understanding the spatio-temporal patterns of consumptive water use (CWU) is one of the most suitable options for formulating the optimal water allocation plans with available water resources under changing climate (Liaqat *et al.* 2015; Azmat *et al.* 2016).

CWU is generally known as the water footprint or virtual water content in the form of actual evapotranspiration (ET_a) (Eriyagama *et al.* 2014). CWU is a key component for simulating hydrological cycles and scheduling irrigation water demands in the agricultural fields. It is known as a complex physical process of land atmosphere interaction which is normally influenced by various hydrometrological conditions such as solar radiation, and land surface characteristics (Allen *et al.* 1998). The complex ecosystem and vegetation heterogeneity makes it difficult to

doi: 10.2166/nh.2016.102

estimate CWU accurately. Knowledge of accurate CWU at the regional scale requires detailed information on various composite elements such as cropping patterns, climatic parameters, hydraulic properties of underlying soils and irrigation practices (Gowda *et al.* 2008; Li *et al.* 2009). The accurate assessment of these composite elements is of paramount importance as these parameters vary significantly both in space and time for large irrigation schemes.

CWU has been traditionally quantified by multiplying the reference evapotranspiration (ET_o) estimated from weather stations with crop coefficient values at field scale (Allen *et al.* 1998). Several other conventional techniques exist for computation of CWU as a point measurement using a lysimeter approach, Energy Balance Bowen Ratio and Eddy Covariance (EC) systems, and water balance establishment over the entire basin (Gowda *et al.* 2008; Li *et al.* 2009; Corbari *et al.* 2014). A number of scientific limitations make it difficult to extrapolate these point scale measurements to large spatial scale (Liaqat *et al.* 2015). In past decades, substantial efforts have been made to retrieve CWU primarily from remote sensing datasets at various spatio-temporal scales. The major benefit of remote sensing based methods is that the CWU can be derived directly as a residual of energy balance which excludes the need of quantification of other complex hydrological processes (Byun *et al.* 2014). However, the difficulties associated with the aforementioned composite elements and underlying heterogeneous irrigation conditions, especially in arid to semi-arid regions of the world, makes it extremely difficult to rely on a single method. Moreover, these methods cannot simulate the impact of climate change on CWU. The soil and water assessment tool (SWAT; Arnold *et al.* 1998), on the other hand, is a physical-based, semi-distributed model which has the capability of predicting the effects of climate change on water balance components.

The Lower Chenab Canal (LCC) irrigation scheme of the large Indus basin irrigation system (IBIS), used in this study, is facing poor conditions for crop production due to major challenges of limiting water resources, primarily caused by inefficient water use, groundwater depletion, climate change, and rapid urbanization and population growth among several other factors (Laghari *et al.* 2012). As water is a scarce commodity of the Indus basin, there are several provincial, national and trans-boundary conflicts which are ultimately adding to the complexity of managing this scarce resource (Cheema *et al.* 2014). Due to limited water availability, LCC normally experiences the huge difference between available water supplies and potential crop water demand that make the accurate quantification of CWU indispensable. Moreover, high climate sensitivity in the region emphasizes the need for careful planning and monitoring of CWU for sustainable water resources management (Ahmad *et al.* 2009; Liaqat *et al.* 2015). In order to address and meet these challenges of deficit water resources, comprehensive robust counterplans are needed which could utilize spatial modeling approaches for the accurate assessment of CWU, especially for regions with complex and heterogeneous vegetation conditions.

In this study, we therefore selected the SWAT model for the assessment of CWU on monthly, seasonal (*Rabi* – October to March and *Kharif* – April to September) and annual basis for entire LCC irrigation scheme, canal command areas (CCAs) of LCC, and different hydrologic response units. The simulations were performed at grid level in the LCC irrigation scheme from 2005 to 2012. Furthermore the impact of climate change on CWU is also determined from 2013 to 2020. A high spatial resolution land use land cover (LULC) map, required for implementing the SWAT model, was generated using a remote sensing approach. Surface Energy Balance Algorithm (SEBAL) was also used to estimate ET_a in order to calibrate and validate the SWAT model. The outcomes of this study will provide guidelines to the policy makers in the region to maximize crop production based on detailed information of CWU both in time and space and to formulate sustainable policy in view of the given future impact of climate change on CWU.

MATERIAL AND METHODS

Study area

We selected the LCC irrigation scheme for the current study. The LCC is one of the representative irrigation schemes of the IBIS which irrigates around 1.22 million hectares (Mha) of agriculture land. The climate of the region is arid to semi-arid which dictates the need for artificial water supplies. The artificial water supplies are through a network of different canals including Sagar, Upper Gugeera, Rakh,

Mian Ali, Jhang, Lower Gugeera, and Burala (Figure 1). Major cropping rotations in the region are cotton–wheat, rice–wheat, sugarcane, and a mix of vegetables. The climate in the region has two major crop seasons, i.e. *Rabi* and *Kharif*. Further details of the study region are presented in Awan & Ismaeel (2014).

Estimating CWU by SWAT

SWAT (Arnold *et al.* 1998), developed by the United States Department of Agriculture – Agricultural Research Service, is a river basin, daily time step operated, continuous time simulated model. It has been extensively used in several recent studies related to land and water resources management (Chung *et al.* 2010; Xie & Cui 2011; Yongwei *et al.* 2012; Singh *et al.* 2015) for successfully quantifying the impact of various management strategies involved in basin hydrology such as LULC, irrigation practices, and changes in reservoir and fertilizer management (Neitsch *et al.* 2005). One of the important outputs of the SWAT modelling is the estimation of water balance after reliable determination of ET_a (Arnold *et al.* 1998, 2012). The water balance equation of soil moisture that represents the hydrologic cycle simulated in SWAT can be expressed mathematically as (Neitsch *et al.* 2005):

$$SW_t = SW_0 + \sum_{i=1}^{t} (P - Q_f - ET_a - W - Q_g) \quad (1)$$

where SW_t is the soil water content at time t (mm), SW_0 is the initial soil water content on day i (mm), t is the time (days), Q_g is the return flow on day i (mm), W is the water entering the vadose zone from the soil profile on day i (mm), ET_Q is the evapotranspiration on day i (mm), Q_f is the surface runoff on day i (mm), P is the amount of rainfall on day i (mm). The open source SWAT theoretical manual 2005 is available for a detailed description of the process involved in this model (Neitsch *et al.* 2005).

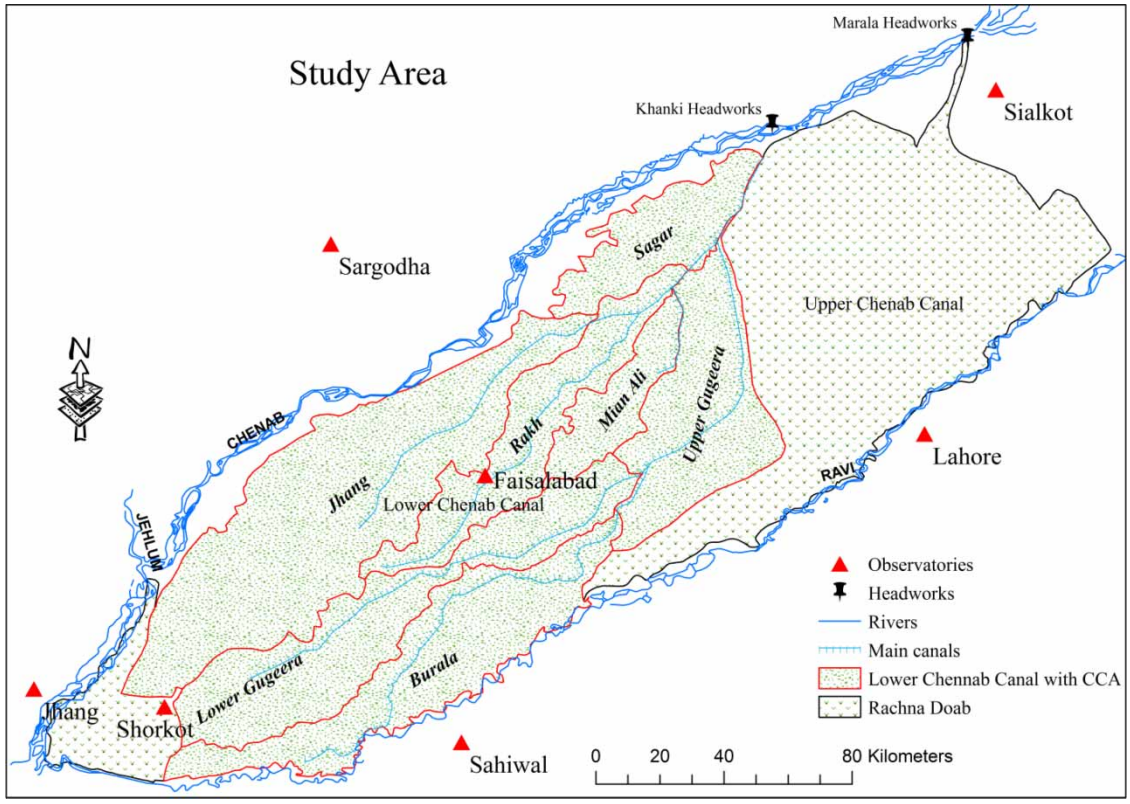

Figure 1 | Geographical location of the LCC irrigation scheme in the Punjab province of Pakistan.

Analytical framework of SWAT model

A good controlling scheme is always essential to obtain accurate simulations from SWAT at the field to regional scale. An analytical framework of SWAT model application for the estimation of CWU is shown in Figure 2. This generally includes the acquisition of quality controlled datasets including pre-processing and final input data preparation according to SWAT model setup.

The basic datasets requirement for SWAT includes information on surface topography, soil features, LULC classification, meteorological parameters and stream flow series (Table 1). A freely available 90 m resolution digital elevation model (DEM) from the Shuttle Radar Topography Mission (SRTM) project governed by US National Aeronautics and Space Administration (NASA) was used in this study to classify the underlying terrain characteristics. A digital soil map generated by the Water and Soil Investigation Division (WASID) of Pakistan was used after the simple classification of soil properties for the study region. In addition to the database of soil properties, the hydrological parameters for different sub-catchments are simulated in SWAT by utilizing the predefined LULC classes (Luzio *et al.* 2002). The predefined sub-catchments in the LCC irrigation scheme were used for delineation by considering LCC as an artificial watershed. Seven sub-catchments in LCC are the original routing of available canal networks, i.e. CCAs of branch canals described above under 'Study area' (Figure 1). Daily stream flow records at the head of each of the seven branch canals covering a time span of

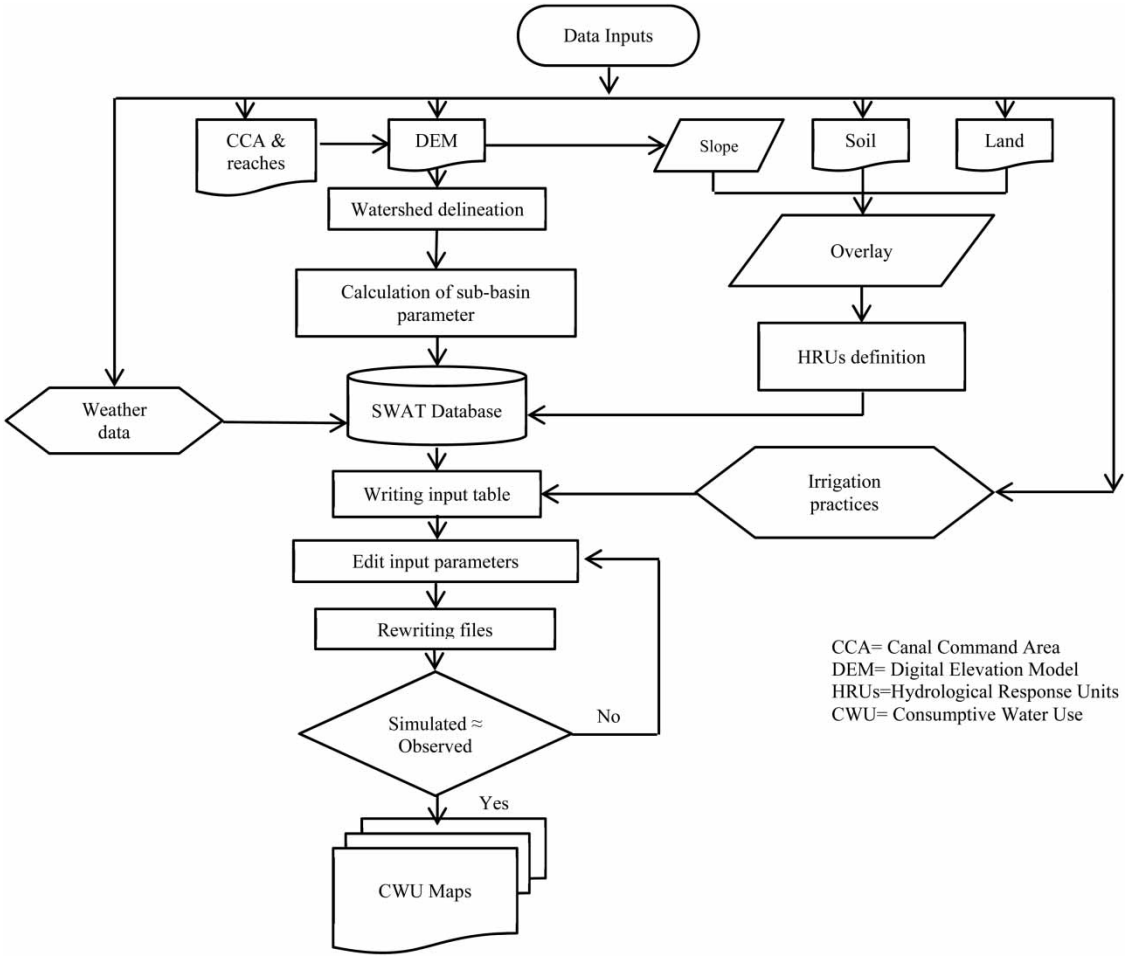

Figure 2 | Flow chart summary describing the detailed methodological framework of the SWAT modelling approach (Awan & Ismaeel 2014).

Table 1 | Description of dataset used in this study

Model	Variables	Spatial resolution	Temporal resolution	Source
SWAT	DEM	90 m	–	SRTM, NASA
	Soil series map	500 m	–	WASID, Pakistan
	LULC classes	250 m	Annual	Awan & Ismaeel (2014)
	Stream flow discharge	Canal head	Daily	PMIU-PID, Pakistan
	Meteorological variables	Stations	Daily	PMD, Pakistan
SEBAL	Surface Albedo	1,000 m	8-day	MODIS
	Vegetation indices	1,000 m	16-day	MODIS
	Emissivity	1,000 m	Instantaneous	MODIS
	Land surface temperature	1,000 m	Instantaneous	MODIS
	Meteorological variables	Stations	Hourly and daily	PMD, Pakistan

2005–2012 were collected from the Programme Monitoring and Implementation Unit, Punjab Irrigation Department (PMIU-PID), Pakistan. Discharge data are used as an irrigation source in the SWAT model to devise irrigation scheduling for different crops on the basis of depth over area ratio. In addition, daily climatic records (2005–2012) of minimum and maximum air temperature, precipitation, wind speed, relative humidity, and solar radiation converted from sunshine duration were obtained from the Pakistan Metrological Department (PMD). These climatic variables are generally used for the estimation of reference ET in SWAT model (Xie & Cui 2011).

An up-to-date LULC map available from a recent study (Awan & Ismaeel 2014) on ground water recharge in LCC irrigation scheme was used in SWAT model simulations. They used the moderate-resolution imaging spectroradiometer (MODIS) products of normalized difference vegetation index (NDVI) for identification of different land cover classes using phonological approaches with high accuracy. In comparison to the ground-based data collected through field surveys from entire LCC irrigation scheme, they reported about 80% accuracy for 12 different LULC classes obtained at 250 m spatial and 8-day temporal resolution by using combined NDVI data of aqua and terra satellites of MODIS. The dominant cropping patterns in the LCC area are wheat-fodder, fodder-fallow, wheat-rice and fodder-maize with relative proportional coverage of approximately 28%, 15%, 12% and 11%, respectively. The other classes such as forest, orchards, natural grass, water and bare or urban settlements constitutes an area of less than 8% of the entire LCC irrigation scheme. Sugarcane is also grown on an area of about 5% specifically in CCA associated with the Jhang branch, while cotton with a rotation of wheat or fodder (14% of the area) is frequently cultivated in Lower Gugeera and Burala CCA. Fodder is the most commonly single grown crop in this region. A similar proportion of different crops as described above was used in the SWAT model for the current study. However, the readers are referred to Awan & Ismaeel (2014) for a further detailed description of the methodology and results of LULC classification.

SEBAL

The SEBAL is a surface energy budget model developed for the estimation of actual evapotranspiration (ET_a) or CWU (Bastiaanssen *et al.* 1998) without using the detailed hydrological characteristics as required in the SWAT model. Although several other remote sensing-based models have been developed in the last few decades for the determination of satellite-based energy budget (Gowda *et al.* 2008; Li *et al.* 2009), SEBAL is the most widely used and validated model in several different regions of the globe, including this study area (Bastiaanssen *et al.* 1998, 2002; Teixeira *et al.* 2009; Awan *et al.* 2011). The extended advantage of SEBAL is that it requires only a limited number of ground-based meteorological data in combination with key input obtained from operationally available satellite images. SEBAL estimates the ET_a as a residual term from the energy budget equation which is expressed as follows:

$$LE = R_N - G_0 - H \quad (2)$$

where R_N is the net radiation absorbed (W/m^2), G_0 is soil heat flux (W/m^2), H is the sensible heat flux (W/m^2) and LE is the latent heat of vaporization (W/m^2) which could readily be converted to ET_a or CWU (Bastiaanssen *et al.* 1998; Karatas *et al.* 2009). In order to solve Equation (2), we used a high temporal resolution MODIS remote sensing dataset covering the same time span from 2005 to 2012 (Table 1). The primary products used in this study included the land surface albedo (MCD43B3), vegetation indices (MOD13A1), emissivity and land surface temperature (MOD11A1) which were freely downloaded from http://glovis.usgs.gov/. In addition to remote sensing-based variables, the hourly and daily climatological parameters such as air temperature, solar radiation, wind speed and relative humidity required in SEBAL were collected from widespread meteorological stations operated by the Pakistan Meteorological Department. A further detailed description of SEBAL methodology can be found in several previous publications (Bastiaanssen *et al.* 1998; Conrad *et al.* 2007; Karatas *et al.* 2009; Teixeira *et al.* 2009; Awan *et al.* 2011). However, the estimations from the SEBAL model in this study were used to calibrate and validate the simulation of SWAT model.

RESULTS AND DISCUSSION

Calibration and validation of SWAT model

In this study, the estimation of CWU by SWAT model were calibrated (2005–2009) based on a trial and error analysis of changing various input parameters to obtain reliable outputs as suggested by Santhi *et al.* (2001). The monthly CWU simulated from the SWAT was compared with SEBAL estimated CWU by means of scatter plot comparison for the accuracy assessment (Figure 3). We adopted the coefficient of determination (R^2), Nash–Sutcliffe model efficiency (NSE), percentage bias (PBIAS) and root mean square error (RMSE), which are commonly used statistical measures for evaluating the predictive performance of SWAT model (Santhi *et al.* 2001; Parajuli *et al.* 2009; Arnold *et al.* 2012). A good agreement was observed in comparison yielding relatively high R^2 of 0.81 and NSE of 0.77 during the calibration process (Figure 3(a)). Previous studies set an

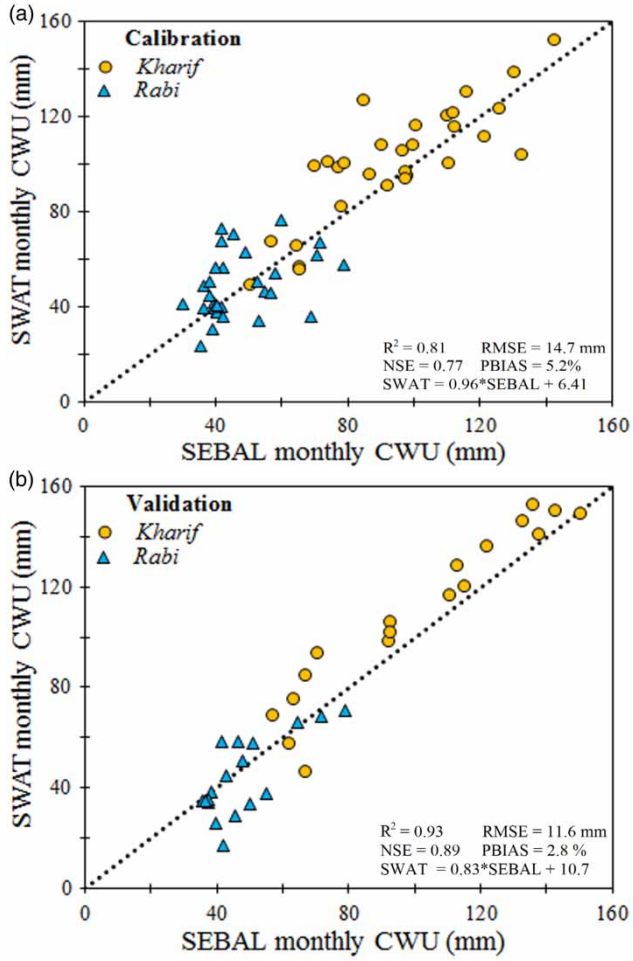

Figure 3 | Statistical comparison between SWAT and SEBAL estimated monthly CWU for the *Rabi* (October–March) and *Kharif* (April–September) seasons during (a) calibration (2005–2009) and (b) validation (2010–2012) periods.

acceptable performance criteria for SWAT with R^2 of 0.60, NSE of 0.50 and difference of ±15% between simulated and reference data (Santhi *et al.* 2001; Arnold *et al.* 2012; Awan & Ismaeel 2014). Thus a difference of less than 6% (PBIAS) between SWAT and SEBAL modelled CWU with RMSE of 14.7 mm at monthly scale provided valuable insights for the hydrological performance of SWAT during the calibration period. It is worth mentioning that the estimations from SEBAL were reliable as this model is extensively established and validated in this study area as well as in several other regions of the world (Bastiaanssen *et al.* 2002; Teixeira *et al.* 2009; Awan *et al.* 2011; Awan & Ismaeel 2014).

The calibrated SWAT model with the same environment was run for another period of 3 years (2010–2012) to

validate the results. Figure 3(b) shows that the intercept value (0.83) between model estimations is slightly decreased compared to those obtained during the calibration (Figure 3(a)) period (0.96). However, the remaining statistics during the validation period was relatively better yielding high R^2 of 0.93, NSE of 0.89, and RMSE of 12 mm month^{-1} with a PBIAS value of less than 3%. Since the SWAT model is known to perform better in relatively wet conditions with a good quality dataset (Xie & Cui 2011), wet conditions were more prevalent during the selected validation period (2010–2012), as this study region faced two mega floods during 2010 and 2012 due to large numbers of rainfall in the monsoon season (Hashmi *et al.* 2012; Yu *et al.* 2013). This fact is perhaps clear in Figure 3(b) where the scatter points during the *Kharif* season were more aligned with the 1:1 line (Figure 3(b)) compared with those of the *Rabi* season. It also revealed that estimation of CWU from SWAT were slightly larger than SEBAL during the *Kharif* season while most of the CWU values were lower than SEBAL during the *Rabi* season. SEBAL and its similar type of energy budget models such as METRIC are known as sensitive to the hydrological extreme (dry and wet) conditions (Liaqat & Choi 2015), which are generally used for their internal calibration to remove systemic biases. Therefore, a small error in the manual selection of dry and wet anchor pixels could considerably change the final ET_a outputs of the SEBAL model (Long & Singh 2012). This could be one of the reasons for slightly contrasting seasonal results from both SWAT and SEBAL models in the current study. The obtained difference (PBIAS $\leq$5.2%) between SWAT and SEBAL simulations for the entire period was within the allowable limit of $\pm$15% as described above (Arnold *et al.* 2012), thus we used the developed SWAT model to determine the impact of climatological conditions on the variations of water use.

Effect of current metrological variables on CWU in LCC irrigation scheme

Figure 4 presents averaged monthly CWU estimated by the SWAT model during the whole calibration and validation period for the entire LCC irrigation scheme, along with monthly variations in mean air temperature and rainfall. Maximum monthly CWU (~124 mm) was observed during the month of May where mean air temperatures almost reached its peak value (31 °C). In contrast, the relatively high air temperature ($\geq$13 °C) values were noticed during the months of October to December, when the monthly CWU was at its minimum ($\leq$37 mm) which was probably caused by the lowest rainfall volume ($\leq$17 mm) for these particular months. The variations in CWU were not only controlled by air temperature and rainfall amounts but also by other climatological variables such as wind speed, relative sunshine duration and relative humidity (Liaqat *et al.* 2015). The effects of these remaining variables were not examined in this study due to lack of availability of a quality dataset.

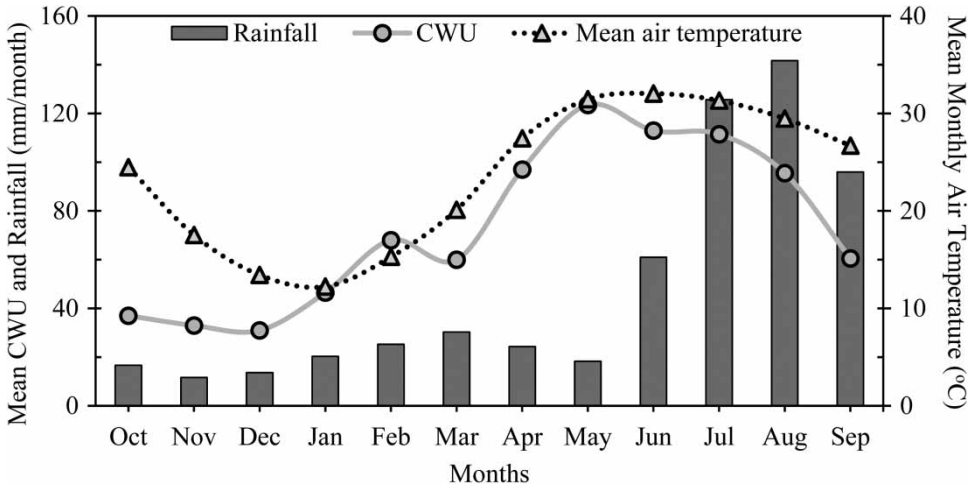

Figure 4 | Time series analysis indicating the variations in average monthly CWU, air temperature and rainfall during the entire study period.

Further, we have determined the significance of air temperature and rainfall corresponding to variations in CWU on a seasonal and annual basis (Table 2). The results showed that the changes in CWU were significantly (p-value <0.05) controlled by the rainfall during the *Rabi* season but by air temperature during the *Kharif* season. The values of Pearson linear correlation, R, were also high (≥ 0.83) for both variables at their significant level. However, the analysis at annual scale revealed that only temperature was significantly impacting the CWU with R values approaching 0.80, while showing non-significant results for rainfall with relatively poor correlation (0.49). The high positive correlation between CWU and air temperature means a high potential of available energy exists in this region to maximally support the vaporous process. In spite of the effects of other factors such as irrigation practices and cropping pattern, this finding indicated the importance of changes in these variables, which in turn largely influence the CWU of large LCC irrigation schemes. Overall, the relatively huge fluctuations in these variables would significantly affect crop production by influencing water demand and supply, and have the capacity to convert a water production area (rainfall > CWU) into a water scarce area (rainfall < CWU).

Spatio-temporal variations in CWU for entire LCC irrigation scheme

The spatial distribution of annual CWU with mean annual averages and standard deviations were mapped for entire LCC irrigation scheme during both the calibration and validation periods (Figure 5). Spatial variations of CWU in LCC ranged from less than 400 mm annum^{-1} to more than 1,100 mm year^{-1}. The low mean CWU values ranging from 786 to 856 mm year^{-1} depicted that relatively drier conditions were more prevalent during the initial period (2005–2006; Figure 5(a) and 5(b)) and the final period (2011–2012; Figure 5(g) and 5(h)) of the study. However, the water use footprints were comparatively high with mean annual CWU varying from 884 to 985 mm year^{-1} and between the periods of 2007–2010 (Figure 5(c)–5(f)). The spatial variation anomalies in CWU represented by means of standard deviations from the averaged CWU values ranged between 72 and 110 mm year^{-1} during both the calibration (2005–2009) and validation (2010–2012) periods. These temporal variations between different years were probably caused by the difference in climatological conditions since irrigation water supplies fulfilled from groundwater (Cheema *et al.* 2014) and cropping patterns or cropping intensities normally remained the same in this study region (Ahmad *et al.* 2009). The lowest values during all the hydrological years were observed in urban areas or those regions where low water requiring crops, such as vegetables, are usually cultivated. Moreover, the low CWU is also distinguishable at the tail end of the LLC irrigation scheme compared with the head end, which is not only caused due to the presence of saline soil and low quality groundwater at the tail end areas of the irrigation scheme but also due to the cultivation of less water demanding crops during the *Rabi* season only. On the other hand, the CCAs such as Sagar, Jhang and lower or upper Gugera branches (see Figure 1), which have high proximity to surface water, showed high CWU values. This was because the high water demanding crops such as rice paddy and

Table 2 | Statistics (Y = ax + b) between SWAT simulated CWU (mm) and meteorological variables on seasonal and annual basis for the entire LCC irrigation scheme

	Rabi (Oct–Mar)		Kharif (Apr–Sep)		Annual	
Statistics	**Rainfall (mm)**	**Mean air temp (°C)**	**Rainfall (mm)**	**Mean air temp (°C)**	**Rainfall (mm)**	**Mean air temp (°C)**
A	1.95	–0.12	–0.16	8.01	0.31	3.34
b	6.57	47.0	109.6	–141.10	55.82	–7.90
R	0.94	0.05	0.39	0.83	0.49	0.79
p-value	0.005[a]	0.95[NS]	0.451[NS]	0.040[a]	0.15[NS]	0.003[a]

p-value with Pearson linear correlation.
NS indicates non-significant difference at the 0.05 probability level.
[a]Indicates significance at the 0.05 probability level.

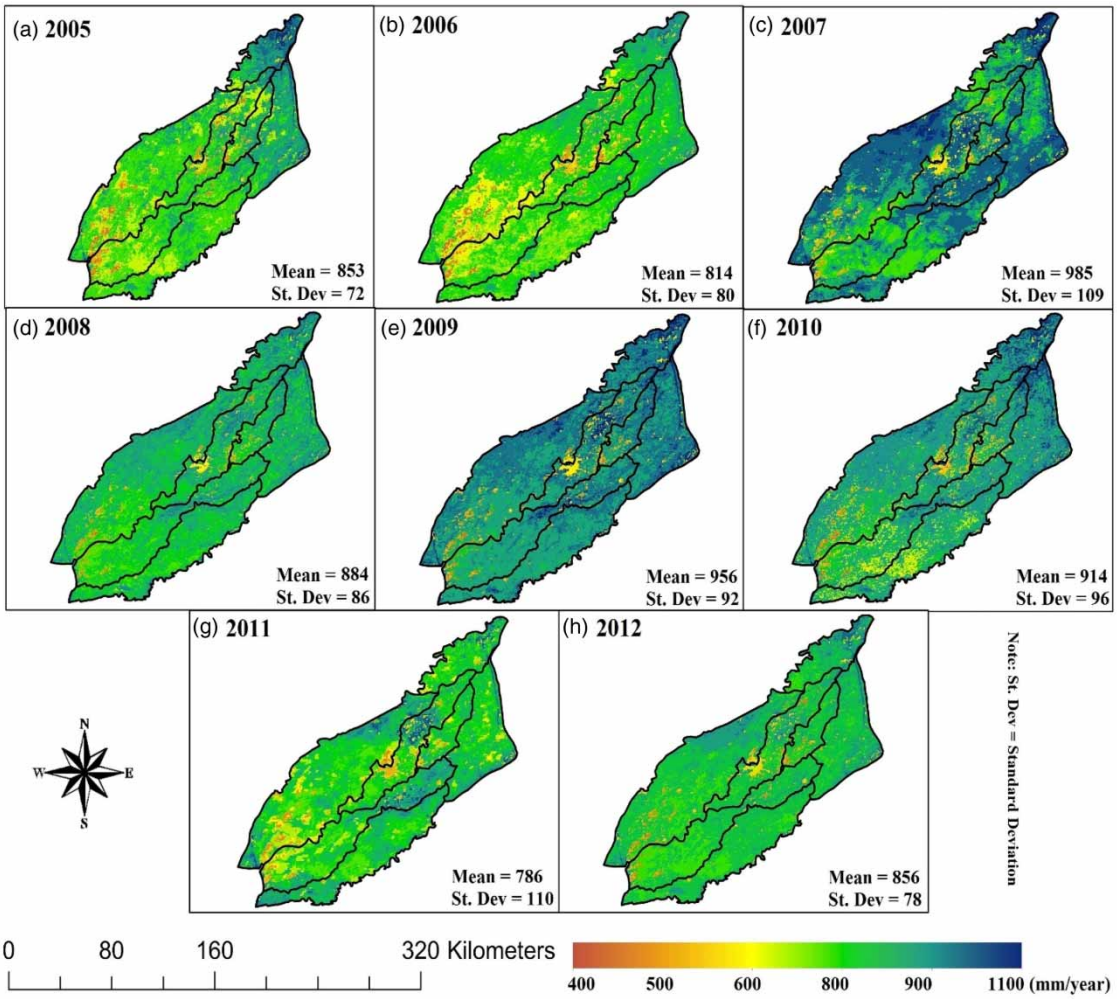

Figure 5 | Spatial distribution of annual CWU during the entire calibration and validation period.

sugarcane are usually grown in these regions during *Kharif* season with a rotation of wheat and other vegetable crops in the *Rabi* season that also causes the difference in water consumption during both cropping seasons.

Effect of changing climate on CWU

CWU from the hydrological operated catchments usually depends upon available irrigation supplies and meteorological conditions as explained above under 'Effect of current metrological variables on CWU in LCC irrigation scheme'. Due to relative homogeneous cropping patterns and system design of the LCC, irrigation water supplies should remain consistent in forthcoming decades. However, the fluctuations in meteorological conditions specifically based on mean precipitation and air temperature could significantly impact the CWU in this region. Based on this assumption, both climatic variables were simulated using Representative Concentration Pathways (RCP 4.5 and RCP 8.5) scenarios for the period 2013–2020 on a daily basis using NorESM global circulation model (Bentsen *et al.* 2013). We reported a decrease of –11% using RCP 4.5 and an increase of 3% using RCP 8.5 for temperature while an increase of 70–75% in rainfall was observed under both scenarios (RCP 4.5 and RCP 8.5) compared with the reference values of the LCC region in our previous study (Awan & Ismaeel 2014). In order to determine the future impacts of climate change on CWU in this study, the

SWAT model was also implemented by using future scenario simulations of rainfall and air temperature from 2013 to 2020 while other variables in SWAT parameterization were kept similar as used during the calibration and validation period (2005–2012). The response of SWAT outputs to future simulated variables was analyzed on a monthly and annual scale.

Climate change scenarios effect on monthly scale in entire LCC irrigation scheme

The average monthly changes in CWU would range from –40 to 67% under RCP 4.5 and from –17 to 80% under the RCP 8.5 scenario compared with the reference values during the validation period (Table 3). The maximum increase (>60%) in CWU would occur during the months of October and November for both scenarios. This increase could be attributed to the observed regional climate shifts that gradually changes the cycle of cool and warm conditions, which in turn could largely disturb the atmospheric system and global energy budget cycle (Ravelo *et al.* 2004). During the hot months (May–August) of *Kharif* season, which also represents the period of monsoon, the average monthly CWU would increase more than 100 mm. This increase can be attributed to high rainfall expected during the monsoon period. The decrease in CWU could be generally noticed during the later period of *Rabi* (January–March) or during the starting period of *Kharif* (April–May) season. The highest decreases of –40 and –17% in CWU would occur during February and April for RCP 4.5 and RCP 8.5, respectively. These decreases can be due to low rainfall and temperature values in these months. Overall, the results simulated from SWAT in this study showed that the annual average CWU would be 76 and 79 mm under RCP 4.5 and RCP 8.5 scenarios which would be approximately 7% and 11% higher by the end of 2020 than the actual CWU simulated during the validation period, respectively.

Table 3 | Mean monthly variations in CWU (mm) for entire LLC irrigation scheme during calibration, validation and for future scenarios under RCP 4.5 and RCP 8.5 simulations

			Scenario period	
Months	Calibration period 2005–2009	Validation period 2010–2012	RCP 4.5 (2013–2020, with % change)	RCP 8.5 (2013–2020, with % change
Oct	35	39	65 (66.7)	69 (76.9)
Nov	36	30	49 (63.3)	54 (80.0)
Dec	36	26	37 (42.3)	40 (53.8)
Jan	46	47	38 (–19.1)	49 (4.30)
Feb	66	70	42 (–40.0)	59 (–15.7)
Mar	67	53	52 (–1.90)	61 (15.1)
Apr	94	100	82 (–18.0)	83 (–17.0)
May	131	116	114 (–1.70)	109 (–6.01)
Jun	116	110	120 (9.10)	107 (–2.70)
Jul	123	100	115 (15.0)	116 (16.0)
Aug	88	103	110 (6.80)	110 (6.80)
Sep	59	62	89 (43.5)	89 (43.5)
Average	75	71	76 (6.7)	79 (10.6)

Climate change scenarios effect on annual scale in different CCAs

Figure 6 and Table 4 represent the impact of climate change scenarios on annual CWU. The averaged spatial variations of CWU during the period of 2013–2020 (Figure 6) under both climate change scenarios showed strong contrasting patterns with 32 mm larger CWU under RCP 8.5 (946 ± 102) compared with those values that obtained for RCP 4.5 (912 ± 80). An entirely different performance of SWAT was observed when the changes in annual CWU were aggregated according to different CCAs in the LCC irrigation scheme (Table 4). This could probably be caused by the difference in available water supplies, underlying soil types, atmospheric conditions and cropping or cultivation practices. Highest annual CWU of 969 mm and 1,001 mm was observed for sagar CCA which showed an increase of 11% and 15% under RCP 4.5 and RCP 8.5, respectively, compared with values of validation period. This is due to the geographical location of the sagar CCA which lies at the head of the water stream, along with cultivation of rice paddy crops and its large proportion of rainfall. The only decrease of about –1% in CWU would occur in the Jhang branch under RCP 4.5, which also showed a minimum increase of about 3% CWU considering the data from RCP 8.5. All other CCAs such as Mian Ali, Upper or Lower Gugeera, Rakh and Burala showed a marginal increase in

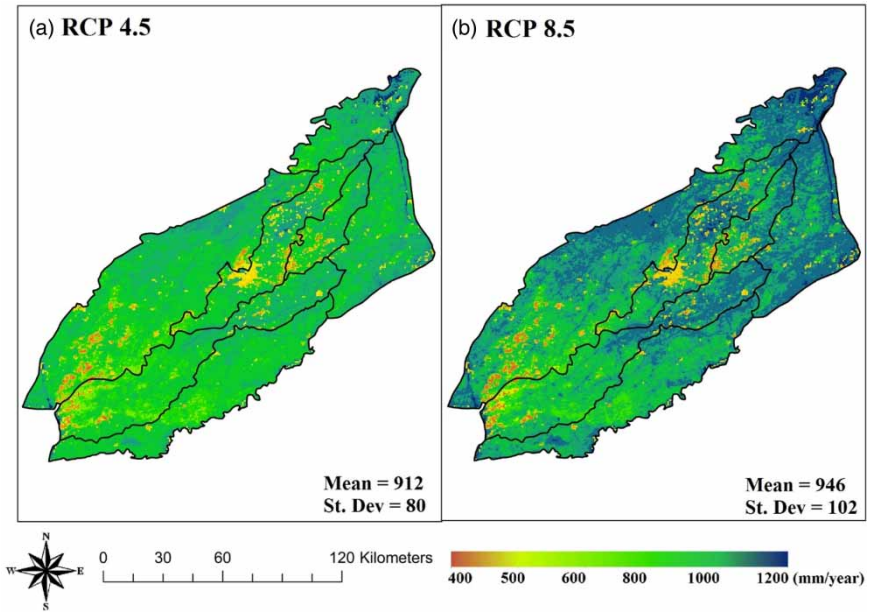

Figure 6 | Spatial variation of average annual CWU (2013–2020) in the LCC irrigation scheme under climate change scenarios (a) RCP 4.5 and (b) RCP 8.5.

Table 4 | Mean annual CWU (mm) during calibration, validation and for future scenarios under RCP 4.5 and RCP 8.5 simulation for seven different CCAs in LCC irrigation scheme

			Scenario period	
CCAs	Calibration period 2005–2009	Validation period 2010–2012	RCP 4.5 (2013–2020, with % change)	RCP 8.5 (2013–2020, with % change)
Sagar	932	866	969 (11.9)	1,001 (15.5)
Mian Ali	826	792	839 (6.0)	873 (10.2)
Upper Gugeera	926	876	946 (8.0)	980 (11.8)
Rakh	806	769	830 (7.9)	862 (12.2)
Jhang	892	889	881 (–0.90)	914 (2.80)
Lower Gugeera	931	879	949 (8.0)	986 (12.2)
Burala	968	894	972 (8.8)	1,009 (12.9)
Average	897	852	912 (6.7)	946 (11.1)

CWU which typically would increase from 5 to 13% by the end of 2020. The lowest annual CWU values for all calibration, validation and for both future scenarios were observed in the Rakh branch which could be due to low cropping intensities in this area and the presence of those soil types which had less capacity to hold the available water (Ahmad *et al.* 2009; Awan & Ismaeel 2014).

CONCLUSIONS

The methodology proposed in this study successfully demonstrated the use of a hydrological model and satellite remote sensing for not only assessing the current use of available water resources for agriculture in large irrigated areas, but also to assess the impact of climate change on CWU in the LLC area of the Indus basin. The SWAT model was successfully calibrated and validated with CWU determined by SEBAL ($R^2 = 0.87 \pm 0.06$, NSE $= 0.83 \pm 0.06$). Results of the modelling on a mean monthly basis during the base period shows that the maximum and minimum CWU are 124 mm and 30 mm during the months of May and December, respectively. This variation in CWU, especially during the *Rabi* and *Kharif* seasons, is due to changes in those climatic parameters which directly influence the CWU.

The correlation of CWU with rainfall and air temperature for the base period showed that the CWU is significantly controlled by rainfall during the *Rabi* season, whereas temperature has a significant impact on CWU during the *Kharif* season. Moreover, CWU varies in space with the lowest and highest values of 400 mm year^{-1} and 1,100 mm year^{-1} at the tail and head end reaches of the

LCC, respectively. Results of the SWAT modelling for a climate change scenario showed that the annual water consumption in the basin would increase overall by approximately 7% and 11% at the end of 2020 under RCP 4.5 and RCP 8.5 climate change scenarios, respectively. The monthly variations would be –40% to 60% and –17% to 80% in both scenarios. The maximum increase (>60%) in CWU would occur during October and November whereas the highest decrease of –40% and –17% in CWU would occur during February and April for RCP 4.5 and RCP 8.5, respectively. The demonstrated results and methodology could be of great value for the policy makers in the region for optimum management of surface and groundwater resources under changing climate.

ACKNOWLEDGEMENTS

The International Water Management Institute (IWMI) is in receipt of financial support from the Embassy of the Kingdom of Netherlands, Islamabad, Pakistan through Grant #22294 and the CGIAR Research Program on Water, Land and Ecosystems (WLE) which were used in part to support this study. The first author was supported through a grant for PhD studies by the Higher Education Commission (HEC), Pakistan. The authors are also grateful to the anonymous reviewers for their valuable suggestions to improve the quality of our manuscript.

REFERENCES

Ahmad, M.-u-D., Turral, H. & Nazeer, A. 2009 Diagnosing irrigation performance and water productivity through satellite remote sensing and secondary data in a large irrigation system of Pakistan. *Agric. Water Manage.* **96** (4), 551–564.

Allen, R. G., Pereira, L. S., Raes, D. & Smith, M. 1998 Crop evapotranspiration – guidelines for computing crop water requirements. FAO Irrigation and Drainage Paper No. 56. FAO, Rome, 300 pp.

Arnold, J. G., Srinivasan, R., Muttiah, R. S. & Williams, J. R. 1998 Large area hydrologic modeling and assessment part I: model development. *J. Am. Water Resour. Assoc.* **34**, 73–89.

Arnold, J., Moriasi, D., Gassman, P., Abbaspour, K., White, M., Srinivasan, R., Santhi, C., Harmel, R., Van Griensven, A. & Van Liew, M. 2012 SWAT: model use, calibration, and validation. *Trans. ASABE* **55** (4), 1491–1508.

Awan, U. K. & Ismaeel, A. 2014 A new technique to map groundwater recharge in irrigated areas using a SWAT model under changing climate. *J. Hydrol.* **519**, 1368–1382.

Awan, U. K., Tischbein, B., Conrad, C., Martius, C. & Hafeez, M. 2011 Remote sensing and hydrological measurements for irrigation performance assessments in a water user association in the lower Amu Darya River Basin. *Water Resour. Manage.* **25** (10), 2467–2485.

Azmat, M., Choi, M., Kim, T.-W. & Liaqat, U. W. 2016 Hydrological modeling to simulate streamflow under changing climate in a scarcely gauged cryosphere catchment. *Environ. Earth Sci.* **75** (3), 186.

Bastiaanssen, W., Menenti, M., Feddes, R. & Holtslag, A. 1998 A remote sensing surface energy balance algorithm for land (SEBAL). 1. Formulation. *J. Hydrol.* **212**, 198–212.

Bastiaanssen, W. G., Ahmad, M. u. D. & Chemin, Y. 2002 Satellite surveillance of evaporative depletion across the Indus basin. *Water Resour. Res.* **38** (12), 1273.

Bentsen, M., Bethke, I., Debernard, J., Iversen, T., Kirkevåg, A., Seland, Ø., Drange, H., Roelandt, C., Seierstad, I. & Hoose, C. 2013 The Norwegian Earth System Model, NorESM1-M – Part 1: Description and basic evaluation of the physical climate. *Geosci. Model Dev.* **6** (3), 687–720.

Brown, M. E. & Funk, C. C. 2008 Food security under climate change. *Sciences* **319**, 580–581.

Byun, K., Liaqat, U. W. & Choi, M. 2014 Dual-model approaches for evapotranspiration analyses over homo- and heterogeneous land surface conditions. *Agric. Forest Meteorol.* **197**, 169–187.

Cheema, M., Immerzeel, W. & Bastiaanssen, W. 2014 Spatial quantification of groundwater abstraction in the Irrigated Indus basin. *Groundwater* **52** (1), 25–36.

Chung, I.-M., Kim, N.-W., Lee, J. & Sophocleous, M. 2010 Assessing distributed groundwater recharge rate using integrated surface water-groundwater modelling: application to Mihocheon watershed, South Korea. *Hydrogeol. J.* **18** (5), 1253–1264.

Conrad, C., Dech, S. W., Hafeez, M., Lamers, J., Martius, C. & Strunz, G. 2007 Mapping and assessing water use in a central Asian irrigation system by utilizing MODIS remote sensing products. *Irrig. Drain. Syst.* **21** (3–4), 197–218.

Corbari, C., Mancini, M., Su, Z. & Li, J. 2014 Evapotranspiration estimate from water balance closure using satellite data for the Upper Yangtze River basin. *Hydrol. Res.* **45** (4–5), 603–614.

Emam, A. R., Kappas, M. & Hosseini, S. Z. 2015 Assessing the impact of climate change on water resources, crop production and land degradation in a semi-arid river basin. *Hydrol. Res.* **46** (6), 854–870.

Eriyagama, N., Chemin, Y. & Alankara, R. 2014 A methodology for quantifying global consumptive water use of coffee for sustainable production under conditions of climate change. *J. Water Clim. Change* **5** (2), 128–150.

Godfray, H. C. J., Beddington, J. R., Crute, I. R., Haddad, L., Lawrence, D., Muir, J. F., Pretty, J., Robinson, S., Thomas, S. M. & Toulmin, C. 2010 Food security: the challenge of feeding 9 billion people. *Science* **327** (5967), 812–818.

Gowda, P. H., Chavez, J. L., Colaizzi, P. D., Evett, S. R., Howell, T. A. & Tolk, J. A. 2008 ET Mapping for agricultural water management: present status and challenges. *Irrig. Sci.* **26** (3), 223–237.

Hashmi, H. N., Siddiqui, Q. T. M., Ghumman, A. R., Kamal, M. A. & Mughal, H. 2012 A critical analysis of 2010 floods in Pakistan. *Afr. J. Agric. Res.* **7** (7), 1054–1067.

Karatas, B. S., Akkuzu, E., Unal, H. B., Asik, S. & Avci, M. 2009 Using satellite remote sensing to assess irrigation performance in water user Associations in the Lower Gediz Basin, Turkey. *Agric. Water Manage.* **96** (6), 982–990.

Laghari, A., Vanham, D. & Rauch, W. 2012 The Indus basin in the framework of current and future water resources management. *Hydrol. Earth Syst. Sci.* **16**, 1063–1083.

Li, Z.-L., Tang, R., Wan, Z., Bi, Y., Zhou, C., Tang, B., Yan, G. & Zhang, X. 2009 A review of current methodologies for regional evapotranspiration estimation from remotely sensed data. *Sensors* **9** (5), 3801–3853.

Liaqat, U. W. & Choi, M. 2015 Surface energy fluxes in the Northeast Asia ecosystem: SEBS and METRIC models using Landsat satellite images. *Agric. Forest Meteorol.* **214–215**, 60–79.

Liaqat, U. W., Choi, M. & Awan, U. K. 2015 Spatio-temporal distribution of actual evapotranspiration in the Indus basin irrigation system. *Hydrol. Process.* **29** (11), 2613–2627.

Long, D. & Singh, V. P. 2012 A modified surface energy balance algorithm for land (M-SEBAL) based on a trapezoidal framework. *Water Resour. Res.* **48** (2), W02528.

Luzio, M., Srinivasan, R. & Arnold, J. G. 2002 Integration of watershed tool and SWAT model into basins. *JAWRA J. Am. Water Resour. Assoc.* **38**, 1127–1141.

Neitsch, S., Arnold, J., Kiniry, J., Srinivasan, R. & Williams, J. 2005 *Soil and Water Assessment Tool Input/Output File Documentation, Version 2005*. USDAARS Grassland, Soil and Water Research Laboratory, Temple, Texas. http://swat.tamu.edu/media/1291/swat2005io.pdf.

Parajuli, P. B., Mankin, K. R. & Barnes, P. L. 2009 Source specific fecal bacteria modeling using soil and water assessment tool model. *Bioresour. Technol.* **100** (2), 953–963.

Ravelo, A. C., Andreasen, D. H., Lyle, M., Lyle, A. O. & Wara, M. W. 2004 Regional climate shifts caused by gradual global cooling in the Pliocene epoch. *Nature* **429** (6989), 263–267.

Santhi, C., Arnold, J. G., Williams, J. R., Dugas, W. A., Srinivasan, R. & Hauck, L. M. 2001 Validation of the SWAT model on a large river basin with point and nonpoint sources. *J. Am. Water Resour. Assoc.* **37**, 1169–1188.

Singh, H. V., Kalin, L., Morrison, A., Srivastava, P., Lockaby, G. & Pan, S. 2015 Post-validation of SWAT model in a coastal watershed for predicting land use/cover change impacts. *Hydrol. Res.* **46** (6), 837–853.

Teixeira, A. d. C., Bastiaanssen, W., Ahmad, M.-u-D. & Bos, M. 2009 Reviewing SEBAL input parameters for assessing evapotranspiration and water productivity for the low-middle São Francisco River basin, Brazil: Part A: calibration and validation. *Agric. Forest Meteorol.* **149** (3), 462–476.

Xie, X. & Cui, Y. 2011 Development and test of SWAT for modeling hydrological processes in irrigation districts with paddy rice. *J. Hydrol.* **396** (1), 61–71.

Yang, W., Andreasson, J., Graham, P., Olsson, J., Rosberg, J. & Wetterhall, F. 2010 Distribution-based scaling to improve usability of regional climate model projections for hydrological climate change impacts studies. *Hydrol. Res.* **41** (3–4), 211–229.

Yang, C., Yu, Z., Hao, Z., Zhang, J. & Zhu, J. 2012 Impact of climate change on flood and drought events in Huaihe River Basin, China. *Hydrol. Res.* **43** (1–2), 14–22.

Yongwei, G., Zhenyao, S., Ruimin, L., Qian, H. & Xing, W. 2012 A comparison of single- and multi-gauge based calibrations for hydrological modeling of the Upper Daning River Watershed in China's Three Gorges Reservoir Region. *Hydrol. Res.* **43** (6), 822–832.

Yu, W., Yang, Y.-C., Savitsky, A., Alford, D., Brown, C., Wescoat, J. & Debowicz, D. 2013 *The Indus Basin of Pakistan: The Impacts of Climate Risks on Water and Agriculture*. World Bank Publications, Washington, DC.

First received 30 April 2015; accepted in revised form 10 November 2015. Available online 4 January 2016